BIOCHEMISTRY
including biophysical chemistry & molecular biology

Article

pubs.acs.org/biochemistry

Cholesterol-Induced Lipophobic Interaction between Transmembrane Helices Using Ensemble and Single-Molecule Fluorescence Resonance Energy Transfer

Yoshiaki Yano, Kotaro Kondo, Ryota Kitani, Arisa Yamamoto, and Katsumi Matsuzaki*

Graduate School of Pharmaceutical Sciences, Kyoto University, Sakyo-ku, Kyoto 606-8501, Japan

Supporting Information

ABSTRACT: The solvent environment regulates the conformational dynamics and functions of solvated proteins. In cell membranes, cholesterol, a major eukaryotic lipid, can markedly modulate protein dynamics. To investigate the nonspecific effects of cholesterol on the dynamics and stability of helical membrane proteins, we monitored association−dissociation dynamics on the antiparallel dimer formation of two simple transmembrane helices $(AALALAA)_3$ with single-molecule fluorescence resonance energy transfer (FRET) using Cy3B- and Cy5-labeled helices in lipid vesicles (time resolution of 17 ms). The incorporation of 30 mol % cholesterol into phosphatidylcholine bilayers significantly stabilized the helix dimer with average lifetimes of 450−170 ms in 20−35 °C. Ensemble FRET measurements performed at 15−55 °C confirmed the cholesterol-induced stabilization of the dimer (at 25 °C, $\Delta\Delta G_a = -9$ kJ mol^{-1} and $\Delta\Delta H_a = -60$ kJ mol^{-1}), most of which originated from "lipophobic" interactions by reducing helix−lipid contacts and the lateral pressure in the hydrocarbon core region. The temperature dependence of the dissociation process (activation energy of 48 kJ) was explained by the Kramers-type frictional barrier in membranes without assuming an enthalpically unfavorable transition state. In addition to these observations, cholesterol-induced tilting of the helices, a positive $\Delta C_{p(a)}$, and slower dimer formation compared with the random collision rate were consistent with a hypothetical model in which cholesterol stabilizes the helix dimer into an hourglass shape to relieve the lateral pressure. Thus, the liposomal single-molecule approach highlighted the significance of the cholesterol-induced basal force for interhelical interactions, which will aid discussions of complex protein−membrane systems.

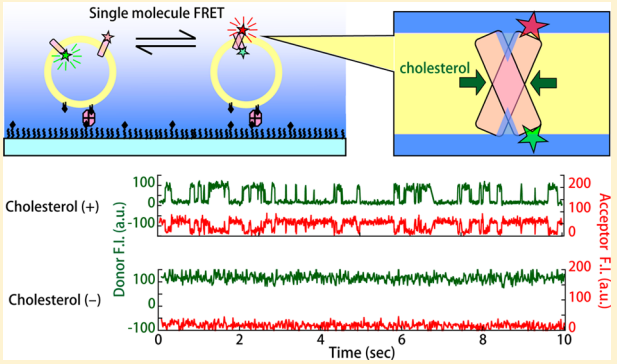

The lipid bilayer environment is a solvent for transmembrane proteins, analogous to an aqueous environment for water-soluble proteins. Therefore, it is essential to consider lipid-derived forces affecting the former to understand their folding and stability,[1−3] like water-originated hydrophobic interaction for the latter, although the general principles of lipid regulation are largely unknown. In contrast to the bulk aqueous phase, the lipid bilayer itself has a supramolecular structure composed of amphiphilic lipids to minimize the energy in the aqueous phase, driven by hydrophobic interactions. Therefore, the anisotropic characters of bilayers, such as restricted lipid orientation and a depth-dependent gradient in hydrophobicity, should lead to distinct constraints on the stability of the incorporated proteins.[4]

Cholesterol, an essential component of eukaryotic membranes, is known to modulate the function and stability of various membrane proteins.[5−9] Plasma membranes typically contain 25−50 mol % cholesterol,[10] the level of which is tightly controlled among organellar membranes.[11] The rigid sterol backbone and small headgroup of cholesterol give it unique characteristics, such as the formation of liquid-ordered domains with phospholipids and a higher lateral pressure in the hydrocarbon core region.[10,12−14] The effects of cholesterol on proteins are both specific and nonspecific and are thus complicated.[1,5,10] Specific interaction motifs have been identified between cholesterol and proteins, suggesting ligand-like effects of cholesterol.[10] The nonspecific bulk phase effects of cholesterol can also be significant; however, little is known about how they influence the thermodynamic and dynamic stability of transmembrane proteins. The purpose of this study was to experimentally elucidate the nonspecific part of cholesterol that has effects on transmembrane helical proteins. Such information will provide a general basis for discussing the effects of lipids on the folding, conformational change, and oligomerization−dissociation processes of membrane proteins in cell membrane environments.

Synthetic transmembrane peptides with naturally occurring and de novo-designed amino acid sequences are useful for investigating protein folding in lipid bilayer environments,[15−20] because transmembrane helical structures can be considered as stable folding units for the formation of tertiary and oligomeric structures.[21,22] According to the model, the thermodynamic

Received: December 16, 2014
Revised: January 21, 2015
Published: January 28, 2015

DOI: 10.1021/bi501528e
Biochemistry 2015, 54, 1371−1379

and dynamic stability of transmembrane proteins should be regulated by lipids through the balance among helix−helix, helix−lipid, and lipid−lipid interactions.[23] In addition to the proximal contact energy, the protein stability is also influenced by geometrical and elastic properties of membranes, such as hydrophobic mismatch[24,25] and the membrane curvature strain.[3,12,26] Indeed, both amino acid sequential motifs[27,28] and lipid compositions[16,18−20] can significantly affect the interhelical interaction.

In this study, we examined a case without sequence motifs to focus on the nonspecific effect of cholesterol, although the sequence motif and lipid composition can exhibit some cooperativity.[29,30] We used the simple de novo-designed transmembrane helix $(AALALAA)_3$, which is devoid of sequence motifs that drive self-association[28,31] such as GXXXG, leucine zipper, and polar interactions and cholesterol binding,[10] e.g., (L/V)-X_{1-5}-Y-X_{1-5}-(R/K), (R/K)-X_{2-6}-(I/V/L)-X_3-(W/Y), and GXXXG. The peptide has been confirmed to assume stable transmembrane helical structures in lipid bilayers with various lipid compositions.[32,33] The helices preferentially form antiparallel dimers because of electrostatic attraction between helix macrodipoles, which was enhanced in thicker membranes with their partial charges at helix termini embedded in a less polar environment. Both hydrophobic mismatch and membrane curvature strain significantly affect the self-association energy of $(AALALAA)_3$ (up to 15 kJ mol^{-1}).[32,33]

The self-association of transmembrane helices in the lipid bilayer environment has been detected by various techniques, including steady state fluorescence,[16,19] steric trap,[20] thiol−disulfide exchange,[18] and biochemical methods.[27,28] However, a bottleneck leads to a limitation of the quantitative measurement of the helix association to obtain thermodynamic and dynamic parameters in lipid bilayer environments. Here, we apply, in addition to ensemble fluorescence resonance energy transfer (FRET), the single-molecule FRET (smFRET) technique[34,35] to directly detect the nonspecific effects of cholesterol on association−dissociation dynamics of the simple transmembrane helices in time scales from milliseconds to seconds. The FRET fluctuations were observed between two transmembrane helices incorporated into large unilamellar vesicles (diameter of ∼100 nm) that were attached to a glass surface.[36] The general driving forces induced by cholesterol will be discussed on the basis of the temperature dependence of helix association.

EXPERIMENTAL PROCEDURES

Materials. Chromophore-labeled peptides for ensemble measurements of X-$(AALALAA)_3$-Y [X = 7-nitrobenz-2-oxa-1,3-diazole (NBD), and Y = NH_2 (**I**); X = Ac, and Y = $NHCH_2CH_2$-S-*N*-(4-{[4-(dimethylamino)phenyl]azo}phenyl)-4′-maleimide (DABMI) (**II**)] were custom-made and characterized by the Peptide Institute (Minoh, Japan). Another labeled pair for single-molecule measurements [X = Cy3B, and Y = NH_2 (**III**); X = Cy5, and Y = NH_2 (**IV**)] was synthesized by the standard 9-fluorenylmethoxycarbonyl (Fmoc)-based method on a NovaSynTGR resin (Millipore, Billerca, MA). Fluorophores were labeled at the N-termini on the resin by treatment with succinimidyl ester derivatives of the fluorophores (2−3 equiv, purchased from GE Healthcare, Little Chalfont, U.K.) in *N*,*N*-dimethylformamide containing 5% *N*,*N*-diisopropylethylamine for 48 h. The peptides were purified by a PLRP-S 300 Å 5 μm reversed phase column (Agilent Technologies, Santa Clara, CA) with an aqueous/acetonitrile gradient containing 0.1% TFA (v/v) at 50 °C and identified by ion spray or matrix-assisted laser desorption ionization mass spectroscopy. The purity of the peptides was higher than 90%. Cholesterol, 1-palmitoyl-2-oleoyl-*sn*-glycero-3-phosphatidylcholine (POPC), and 1,2-dipalmitoyl-*sn*-glycero-3-phosphoethanolamine-*N*-(cap biotinyl) (biotin-PE) were obtained from Avanti (Alabaster, AL). NeutrAvidin was a product of Thermo Scientific (Waltham, MA). Poly(ethylene glycol) (PEG)-coating reagents were obtained from Laysan Bio (Arab, AL). Spectrograde organic solvents were products of Nacalai Tesque (Kyoto, Japan). Other chemicals were obtained from Sigma-Aldrich (St. Louis, MO) unless otherwise stated. Cholesterol and POPC were dissolved in ethanol and chloroform, respectively, and their concentrations were determined in triplicate by the cholesterol oxidase method [Free Cholesterol E-Test kit (Wako, Tokyo, Japan)] and phosphorus analysis,[37] respectively.

FTIR Spectroscopy. Oriented films of lipids and peptides were prepared by uniformly spreading a 100 μL ethanol solution of lipids (5 μmol) and peptides (15 nmol) on a germanium ATR plate (70 mm × 10 mm × 5 mm), followed by evaporation of the solvent with N_2 gas under a vacuum overnight. The films were hydrated with a D_2O-soaked piece of filter paper put over the plate for 3 h at 25 °C. FTIR−PATR measurements were conducted as described previously[33,38] on a Bio-Rad FTS-3000MX spectrometer equipped with a Specac horizontal ATR attachment with an AgBr polarizer and a temperature controller. The dichroic ratio, *R*, defined by $\Delta A_{\parallel}/\Delta A_{\perp}$, was calculated from the polarized spectra. The absorbance (ΔA) was obtained as the area for the amide I band. Subscripts ∥ and ⊥ refer to polarized light with the electric vector parallel and perpendicular to the plane of incidence, respectively. The average helix orientation angle to the bilayer normal, α, was calculated from *R*:

$$\cos^2 \alpha = \frac{1}{3}\left(\frac{4}{3\cos^2 \theta - 1}\frac{R - 2.00}{R + 1.45} + 1\right) \quad (1)$$

We assumed a fixed angle (θ) of 35° between the helix axis and transition moments for amide I bands.[38]

Liposome Preparation. Large unilamellar vesicles (LUVs) were prepared by an extrusion method using a buffer containing 10 mM Tris, 150 mM NaCl, and 1 mM EDTA (pH 7.4) (TE buffer), as described in a previous report.[38] Hydration and extrusion were performed at ∼50 °C to ensure the mixing of membrane components.

Ensemble FRET. The self-association of the helix was determined by FRET from **I** to **II**. Detailed procedures for the measurements and analysis have been described in previous reports[32,33] and are included in the Supporting Information. The temperature dependence of the thermodynamic parameters for the self-association was analyzed by

$$\Delta G = \Delta H + \Delta C_p(T - T_{ref}) - T\Delta S - T\Delta C_p \ln(T/T_{ref}) \quad (2)$$

where T and T_{ref} represent the observed temperature and standard state reference temperature (298 K in this study), respectively.

Single-Molecule FRET. The biotin-PEG-coated slide chamber for fixing LUVs was prepared according to the protocol of Joo and Ha.[39] Briefly, No. 1-S cover glass (Matsunami Glass, Osaka, Japan) was washed with 1 M KOH and methanol, amino-functionalized by aminopropylsi-

DOI: 10.1021/bi501528e
Biochemistry 2015, 54, 1371−1379

lane, and coated with biotinylated PEG by treatment with PEG-succinimidyl ester, with an average MW of 5000 (mPEG-SVA), and its biotin derivative (biotin-PEG-SVA) at a ratio of 80/1 (w/w). The helices labeled with Cy3B (**III**) and Cy5 (**IV**) at the N-termini were incorporated into LUVs (total lipid concentration of 5 mM) at a 1/1/90000/900 **III**/**IV**/lipid/biotin-PE molar ratio. The biotinylated LUVs were diluted to 10 μM lipids, added onto the biotin-PEG-coated glass surface, and incubated for 1 min after a 10 min pretreatment with 0.2 mg mL^{-1} NeutrAvidin. This procedure typically resulted in 200−400 vesicles in the analyzed area (80 μm × 80 μm). The fluorescence images for Cy3B (575−635 nm) and Cy5 (645−745 nm) under Cy3B excitation at 561 nm were simultaneously acquired using an ImagEM EM-CCD camera with W-View optics (Hamamatsu Photonics, Hamamatsu, Japan) under a Nikon (Tokyo, Japan) Ti-based total internal reflection microscope with a time resolution of 17 ms. To suppress photoblinking, the observation was performed in TB buffer containing 1 mM trolox, 1 mM methyl viologen, 0.8% (w/v) D-glucose, 0.25 mg mL^{-1} glucose oxidase, and 10.5 mg mL^{-1} catalase (pH 7.4).[40] The apparent FRET efficiency, E_{app}, was calculated from fluorescence intensities for the donor (F_{Cy3B}) and acceptor (F_{Cy5}) as $E_{app} = F_{Cy5}/(F_{Cy3B} + F_{Cy5})$. The smFRET trajectories originating from the monomer−dimer transitions were analyzed with HaMMy[41] to deduce the rate constants between different states.

RESULTS

Ensemble Measurements. To examine the effects of cholesterol on the behaviors of transmembrane helices, 30 mol % cholesterol was added to the typical phospholipid POPC to prepare POPC/cholesterol membranes. This composition does not exhibit macroscopic phase separation; instead, it has been proposed to submicroscopically demix into l_d and l_o states.[42] The hydrophobic length of helix $(AALALAA)_3$ (27−29 Å)[32] is comparable to the hydrophobic thickness of the bilayers (average distance between carbonyls), although the thickness slightly increases in the presence of cholesterol (3−4 Å) compared with that of pure POPC bilayers (thickness of ∼27 Å) because of acyl chain ordering.[43,44] Before measuring single-molecule kinetics, we examined the ensemble properties of the transmembrane helices by Fourier transform infrared−polarized attenuated total reflection (FTIR−PATR) spectroscopy and fluorescence experiments.

FTIR−PATR spectroscopy was used to confirm the helical structure and transmembrane orientation of the peptides in D_2O-hydrated oriented bilayers on an ATR crystal. Panels a and b of Figure 1 show the amide region spectra for peptide **I** incorporated into membranes (1/333 peptides/lipids, or X_p = 0.006) at 25 °C. X_p is the doubled mole fraction of peptide $X_p = 2n_p/(2n_p + n_l)$, in which n_p and n_l indicate the moles of peptides and lipids, respectively. A factor of 2 was introduced to take the transmembrane nature of the peptide into consideration.[38] In both POPC and POPC/cholesterol bilayers, narrow amide I and II absorption bands were observed (half-width of ∼15 cm^{-1}), suggesting homogeneous secondary structures. The intensity of amide II bands around 1546 cm^{-1} did not decrease significantly even after hydration with D_2O vapor for 3 h, indicating that the helix is buried in the hydrocarbon core of the membrane without H/D exchange. The amide I band in the presence of cholesterol (1663 ± 1 cm^{-1}) was slightly blue-shifted from that in pure POPC (1660 ± 1 cm^{-1}). The average orientation angles of the helix axis to the bilayer normal were

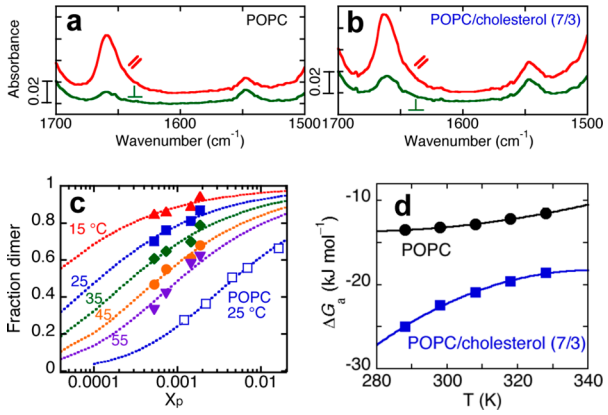

Figure 1. Ensemble properties of transmembrane helix $(LLALAA)_3$. (a and b) Amide region FTIR−PATR spectra measured for **I**/lipid (1/333) films hydrated with D_2O (25 °C). The lipid compositions are shown in the figures. Red and green lines indicate raw spectra for the IR beam with its electric vector parallel and perpendicular to the plane of incidence, respectively. (c) Monomer−dimer equilibrium of the helix in POPC/cholesterol (7/3) bilayers at 15−55 °C (n = 2−4). The fraction dimer is plotted as a function of X_p. Error bars are smaller than the symbols. Dotted lines indicate fitting curves assuming monomer−dimer equilibrium constants, K_a, of 35000 ± 6000, 8650 ± 930, 3560 ± 360, 1650 ± 110, and 920 ± 110 at 15, 25, 35, 45, and 55 °C, respectively. Data in pure POPC at 25 °C are also shown for comparison.[33] (d) Temperature dependence of ΔG_a ($=-RT \ln K_a$). Solid lines denote fitting curves using eq 2 with parameters summarized in Table 1. Data in pure POPC at 25 °C are also shown for comparison.[33]

estimated from the dichroic ratio R ($\Delta A_{\parallel}/\Delta A_{\infty}$) ($n$ = 3). High R values (3.8 ± 0.4) observed for amide I bands in POPC/cholesterol bilayers corresponded to a helix orientation angle of 28 ± 4°. Interestingly, a slight helix tilt was observed in the presence of cholesterol, in contrast to an almost vertical orientation in pure POPC (R = 6.3, and an orientation angle of ∼0°). Similar transmembrane orientations were observed at 5 °C (27 ± 3°) and 55 °C (29 ± 7°) (spectra not shown). Although the secondary structures of the helices were influenced by the incorporation of cholesterol, the helices did not preferentially interact with cholesterol, as confirmed by FRET experiments from fluorescent sterols (dehydroergosterol) to **I** (see Figure 1 of the Supporting Information).

We detected antiparallel dimers in POPC/cholesterol bilayers in a peptide concentration range without self-quenching of NBD attached at the N-terminus of the helix (X_p < 0.002; see Figure 2 of the Supporting Information) because self-quenching suggests associations in a parallel orientation. The upper limit without quenching was 1 order of magnitude lower than that in POPC (X_p < 0.02).[33] The antiparallel dimer was selectively detected by FRET from the donor NBD to the acceptor DABMI attached at the N- and C-termini of the helices, respectively (**I** and **II**), because of a short critical transfer distance (R_0) of 25 Å.[32] Representative fluorescence spectra are shown in Figure 3 of the Supporting Information. The concentration dependencies of dimerization fit well to the theoretical curves assuming a monomer−dimer equilibrium of 15−55 °C (Figure 1c) to yield an association free energy change, ΔG_a (Figure 1d), and other thermodynamic parameters, ΔH_a, ΔS_a, and $\Delta C_{p(a)}$, which are summarized in Table 1. Cholesterol enhanced antiparallel dimer formation of the helix ($\Delta\Delta G_a = -9$ kJ mol^{-1}), with a marked decrease in enthalpy ($\Delta\Delta H_a = -60$ kJ mol^{-1}).

DOI: 10.1021/bi501528e
Biochemistry 2015, 54, 1371−1379

Table 1. Thermodynamic Parameters for Formation of the Antiparallel Dimer of the Helix at 298 K

membrane	ΔG_a (kJ mol^{-1})	ΔH_a (kJ mol^{-1})	$-T\Delta S_a$ (kJ mol^{-1})	$\Delta C_{p(a)}$ (J K^{-1} mol^{-1})
POPC	−13.2 ± 0.2	−23.7 ± 0.4	10.4 ± 0.4	−0.5 ± 0.1
POPC/cholesterol (7/3)	−22.6 ± 0.1	−84.1 ± 1.7	61.4 ± 1.7	1.5 ± 0.3

Single-Molecule Measurements. Single-molecule FRET measurements were performed using the FRET pair, Cy3B (donor) and Cy5 (acceptor), which were attached at the N-termini of the helices (**III** and **IV**) (Figure 2a). Because of the relatively long critical transfer distance for Cy3B and Cy5 (R_0 = 67 Å),[45] the pair can detect both parallel and antiparallel dimers. For single-molecule detection, the sample was prepared such that one vesicle (~9×10^4 lipids) included only two transmembrane helices on average ($X_p \sim 4 \times 10^{-5}$). At that concentration, the formation of antiparallel dimers in POPC/cholesterol bilayers should be significant (~35% at 25 °C), as expected from the ensemble FRET measurements, although that of parallel dimers should not, inferred from the self-quenching experiments (Figure 2 of the Supporting Information). The liposomes were attached on a glass surface via interaction between biotin and avidin.[39] For smFRET measurements, the fluorescence signals from Cy3B (Figure 2b) and Cy5 (Figure 2c) were simultaneously imaged by total internal reflection microscopy under excitation of Cy3B (time resolution of 17 ms). After the measurements, the number of helices was determined by stepwise photobleaching (Figure 2d,e). We selected vesicles that had incorporated only one donor helix and one acceptor helix for smFRET analysis. The helices were randomly incorporated into vesicles because the number distribution of the helices obeyed a Poisson distribution (Figure 4 of the Supporting Information). We also checked the homogeneity of the vesicles in terms of the size and lipid composition by measuring the vesicle size with dynamic light scattering [70−110 nm (data not shown)] and using two fluorescent lipids that partition into l_d and l_o phases, respectively (Figure 5 of the Supporting Information).

In smFRET measurements, dimer formation was detected as a stepwise decrease in donor fluorescence intensity with a concomitant increase in acceptor fluorescence intensity (Figure 2f). Dissociation of the dimer resulted in stepwise recovery of the donor emission and simultaneous disappearance of the acceptor emission. In the presence of cholesterol, roughly half (57%; n = 93) of the selected vesicles exhibited FRET fluctuation trajectories with FRET durations of subseconds (Figure 2f, top traces), whereas the other half did not show detectable FRET signals in the time course (Figure 2f, bottom traces). We interpreted the findings as evidence that dimerization occurred only for helices that had been incorporated into an LUV with an antiparallel orientation and not for those with a parallel orientation.[a] This interpretation was confirmed by smFRET measurements using disulfide-linked dimers fixed in an antiparallel orientation (Figure 6 of the Supporting Information). In this case, FRET fluctuations were observed in most vesicles (86%; n = 28) after reduction of the disulfide bond. In contrast to cholesterol-containing bilayers, no FRET was observed in pure POPC vesicles incorporating donor−acceptor helix pairs (n = 30). Because the ensemble measurements predict that only ~2% of the helices should form dimers under the smFRET condition at 25 °C, it is reasonable to interpret the dimer lifetime as being much shorter than the time resolution even with an antiparallel orientation.

The smFRET experiments in POPC/cholesterol vesicles were performed at 20, 25, 30, and 35 °C (Figure 7 of the Supporting Information). The apparent FRET efficiency, E_{app}, was calculated from fluorescence intensities of the donor, F_{Cy3B}, and the acceptor, F_{Cy5}, for all vesicles containing a donor−acceptor pair (Figure 2g). The histograms were fit with two Gaussian peaks corresponding to the monomer and dimer. The temperature dependence of the fraction dimer (estimated from the relative area of the peak with a higher E_{app}) was explained well by a theoretical curve calculated from thermodynamic parameters determined in the ensemble measurements (Figure 2h). Using all the data, we concluded that the smFRET measurements reliably detected dynamic equilibrium between the helix monomer and antiparallel dimer in cholesterol-containing vesicles.

Kinetic Analysis. Kinetic parameters for formation of the antiparallel dimer and its dissociation into monomers were analyzed vesicle by vesicle on the basis of the hidden Markov model. We used the HaMMy fitting program for smFRET trajectories assuming two-state transitions.[41] The fitting has an advantage over simple threshold analysis in considering the noise-induced E_{app} distribution for each state to resolve state-to-state transitions from noisy trajectories. An example is shown in Figure 3a. The rate constants for dimer formation (k_{on}) (Figure 3b) and dissociation (k_{off}) (Figure 3c) were calculated from the obtained transition probabilities at 20 °C (n = 21), 25 °C (n = 36), 30 °C (n = 29), and 35 °C (n = 30). The ln(k) distributions were fit with Gaussians[41] to obtain the center values and half-widths, which are summarized in panels d and e of Figure 3. The rate constants for dimerization did not exhibit a clear temperature dependence [k_{on} = 6 ± 2 s^{-1} (Figure 3d)], whereas dimer dissociation was enhanced at higher temperatures (k_{off} values of 2.2 ± 1.8 and 5.8 ± 2.5 s^{-1} at 20 and 35 °C, respectively) with an Arrhenius activation energy, $E_{a(off)}$, of 48 ± 3 kJ mol^{-1} (Figure 3e).

DISCUSSION

Although a large number of theoretical and simulation studies have predicted the general importance of membrane physicochemical properties to the stability of membrane proteins,[3] it is not necessarily easy to perform wet experiments to examine the prediction. One obstacle involves experimental limitations on measuring the dynamics of proteins in lipid bilayers. Single-molecule fluorescence microscopy and spectroscopy are well-established techniques not only for detecting conformational changes in purified biomolecules[34,35] but also for tracking the diffusion and oligomerization of membrane proteins in living cell membranes.[46−48] Subsecond dimer lifetimes have been reported for the M1 muscarinic receptor,[46] *N*-formyl peptide receptor,[47] and GPI-anchored proteins.[48] Surprisingly, we found that the lifetime of the transmembrane dimer could be on the order of subseconds even for the simplest transmembrane helices in binary membranes. This result suggests that the nonspecific effects of lipids can be a dominant force for the transient stabilization of transmembrane proteins even in more complex environments. The stability of the cholesterol-

DOI: 10.1021/bi501528e
Biochemistry 2015, 54, 1371−1379

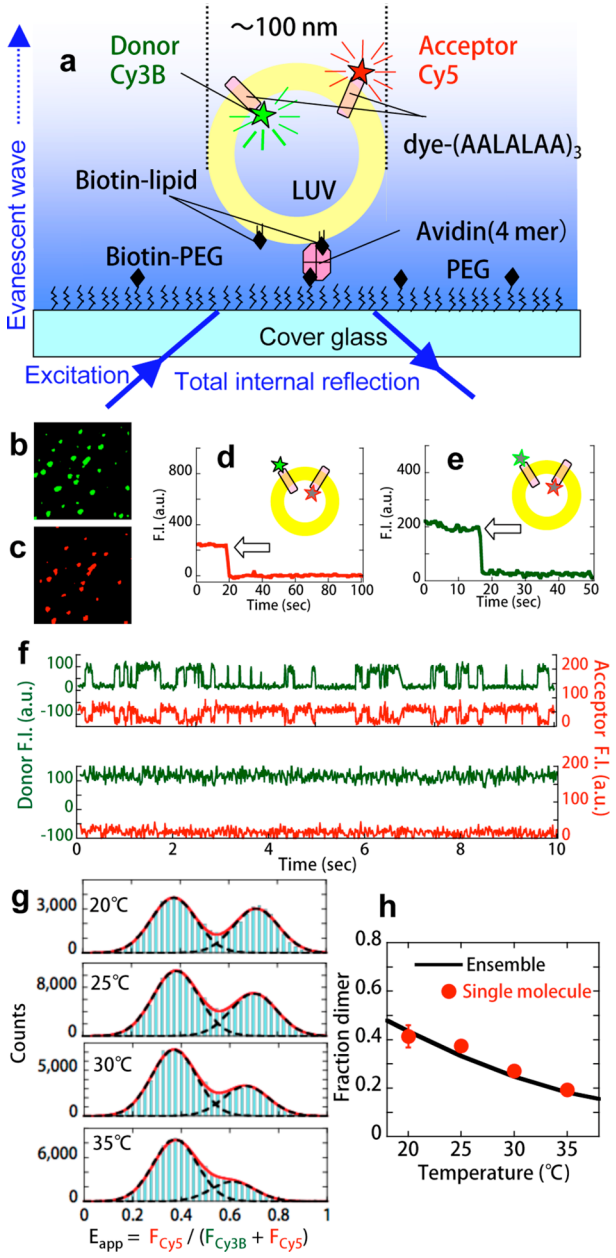

Figure 2. smFRET between two transmembrane helices. (a) Schematic illustration of a surface-attached vesicle for imaging by total internal reflection microscopy. (b and c) Fluorescence images for Cy3B and Cy5, respectively, attached to helices in POPC/cholesterol vesicles (imaged area of 20 μm × 20 μm). (d and e) Photobleaching of Cy5 and Cy3B, respectively, detected as a stepwise decrease in the fluorescence intensities (arrows). (f) Representative time courses of fluorescence intensities for Cy3B (green) and Cy5 (red) under excitation of Cy3B in POPC/cholesterol bilayers at 25 °C. The vesicles that had incorporated one Cy3B helix and one Cy5 helix were selected. The emissions in the top traces fluctuate with an anticorrelation, reflecting the association−dissociation dynamics of the helices, whereas only Cy3B emits in the bottom traces, indicating no association between the helices. (g) Histograms of apparent FRET efficiency, E_{app}, in POPC/cholesterol vesicles. Dimer fractions were estimated from the peak areas by fitting with two Gaussians. (h) Dimer fraction obtained from E_{app} (circles) and ensemble association constants (solid line).

induced dimer will be discussed below from the viewpoints of the structure, energetics, and dynamics.

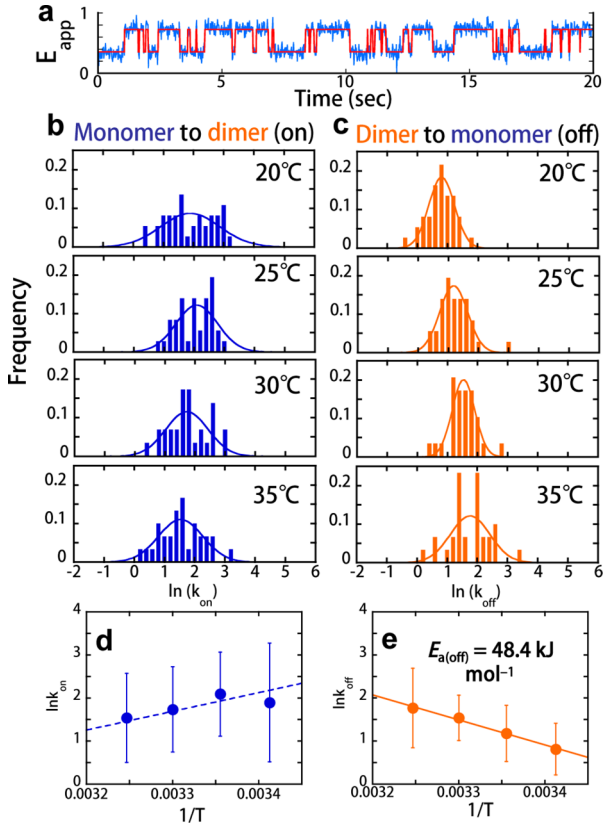

Figure 3. Kinetics of the monomer−dimer transition. (a) Example of E_{app} fluctuations (blue) and fitting using the HaMMy program (red). (b and c) Distributions of rate constants for association and dissociation, respectively. The histograms were fit with Gaussians to estimate the average rate constants. (d and e) Temperature dependencies of rate constants for association and dissociation, respectively. The solid line in panel e indicates linear fitting of the data to estimate the activation energy, $E_{a(off)}$, whereas the dotted line in panel d is a simulation according to eq 4 assuming the constant term to be an adjustable parameter.

Transmembrane Structure. FTIR−PATR measurements have proven the presence of stable transmembrane helical structures of peptide $(AALALAA)_3$ in various lipid bilayers.[32,33] The observed slight blue shift of the amide I band (1663 ± 1 cm^{-1}) in the presence of cholesterol is anticipated for interhelical vibrational coupling because of the oligomerization of helices in membranes.[49] Helix oligomerization under the condition of FTIR measurement (X_p = 0.006) is also consistent with the results of self-quenching (Figure 2 of the Supporting Information) and ensemble FRET measurements (Figure 1c). The observed tilt of the helices in POPC/cholesterol bilayers (25−30°) despite a slight thickening of bilayers indicates that the oligomers are stabilized with a defined crossing angle. A similar helix tilt has been observed in the presence of small-headgroup lipids (1-palmitoyl-2-oleoyl-*sn*-glycero-3-phosphatidylethanolamine).[33] We suggest that the observed tilting is due to the formation of hourglass-shaped dimers to partially compensate for the higher lateral pressures in the bilayer's central region in the presence of POPE or cholesterol (vide infra). Such tilting of the helices is commonly observed in crystal structures of helical membrane proteins.[50]

Association Energetics. Cholesterol enhanced the self-association of $(AALALAA)_3$, consistent with previous observations of various transmembrane sequences.[9,16,18,19] The

DOI: 10.1021/bi501528e
Biochemistry 2015, 54, 1371−1379

cholesterol-induced $\Delta\Delta G_a$ values (7−12 kJ mol^{-1} at 55−15 °C) are comparable to those of multiple H-bonds between transmembrane helices.[51] Fluorescent sterol experiments (Figure 1 of the Supporting Information) suggest that the sterols tend to preferentially interact with POPC and condense the helices into sterol-poor regions. Acyl chain ordering of POPC by cholesterol can also interfere with favorable helix−POPC packing. Similar cholesterol-dependent protein condensation has been reported in complex cell membranes.[52] Our results indicate that such lipid-induced protein concentration can be reproduced even in a binary mixture of POPC and cholesterol. In the following paragraphs, we will discuss possible driving forces for dimerization from the viewpoints of molecular contact energies and bilayer physicochemical properties.

The equation in Figure 4a represents the differences in contact energies upon helix association, in which ΔG_{H-H}, ΔG_{H-L}, and ΔG_{L-L} denote the free energies of helix−helix, helix−lipid, and lipid−lipid interactions, respectively.[23] Removal of n lipids from the helix results in the generation of $n/2$ lipid−lipid contacts. The same relationships hold for other thermodynamic parameters. According to the differences in molecular contact based on the model, stronger helix−helix interactions, weaker helix−lipid interactions, and stronger lipid−lipid interactions are possible causes of helix dimerization (Figure 4a). Helix macrodipole interaction is a basal driving force of helix−helix interaction, the strength of which depends on the polarity of the helix termini and shape of the dimer (Figure 4a).[32,33] In the presence of cholesterol, a slight increase in the hydrophobic thickness (3−4 Å) should strengthen the dipole interaction by lowering the polarity around the helix termini. On the other hand, the helix tilt in hourglass-shaped dimers[33] and a stronger hydration in the headgroup region in cholesterol-containing membranes[53] should attenuate the dipole interaction. A decrease in the terminal dielectric constant from 15 to 8 and an increase in helix tilting from 0° to 25° result in a maximal enthalpic difference of −5 kJ mol^{-1} (−23 to −28 kJ mol^{-1}), which can explain only ∼8% of the observed decrease in $\Delta\Delta H_a$ (−60 kJ mol^{-1}). Therefore, the difference in the macrodipole interaction is not a dominant force that drives the association of the helices. This is consistent with the small $\Delta\Delta G_a$ (−2 kJ mol^{-1} at 25 °C) previously observed for membrane thickening from 27 to 30.5 Å by increasing the PC acyl chain length from diC (18:1) to diC (20:1).[32] A similar thickening effect was assumed for cholesterol-containing membranes [−2 kJ mol^{-1} (Figure 4a)]. Other than the helix−helix interaction, an increase in the level of favorable POPC−cholesterol packing and a decrease in the level of unfavorable POPC−helix packing can decrease the free energy driven by a negative enthalpy (Figure 4a). In previous studies, we estimated these lipid-related contributions from the thermodynamics of intermembrane transfer of the helix,[32,33] although this approach was not applicable here because of the rapid intervesicular transfer of cholesterol. Therefore, the free energy contribution (−2 kJ mol^{-1}) was indirectly estimated as a residual of the other two contributions (Figure 4a). $\Delta C_{p(a)}$ in the presence of cholesterol (1.5 kJ mol^{-1} K^{-1}) was significantly larger than that in POPC (−0.5 kJ mol^{-1} K^{-1}). A similar increase in $\Delta C_{p(a)}$ has been observed by the incorporation of POPE and thickening of membranes.[32,33] Because the positive heat capacity has been reported for the aqueous exposure of nonpolar groups,[54] the observed large $\Delta C_{p(a)}$ can be at least partially explained by the penetration of water molecules into membrane regions upon dimerization. One possibility is the penetration of water between helices[55,56] in the hourglass-shaped dimer. Consistent with this expectation, a large negative association entropy was observed in the presence of cholesterol ($-T\Delta S_a$ = 61 kJ mol^{-1}). Losses of the translational and rotational degrees of freedom (up to 8 kJ mol^{-1}) and a decrease in side chain conformational entropy (up to 22 kJ mol^{-1})[32] can explain only half of the observed entropy, suggesting further configurational restrictions such as hourglass-shaped dimers with penetration of water. An increase in the level of favorable lipid−lipid packing is another possible cause of the decrease in entropy upon helix dimerization.

In addition to the molecular contact energies, another membranous force can originate from the lateral pressure profile (or curvature strain) from the imbalance between cross sections of the headgroup and hydrocarbon core regions (Figure 4a).[3,26] A higher lateral pressure in the hydrocarbon core can be partially released by the formation of an hourglass-shaped dimer. According to a continuum model considering elastic constants for bending and the area expansion of the

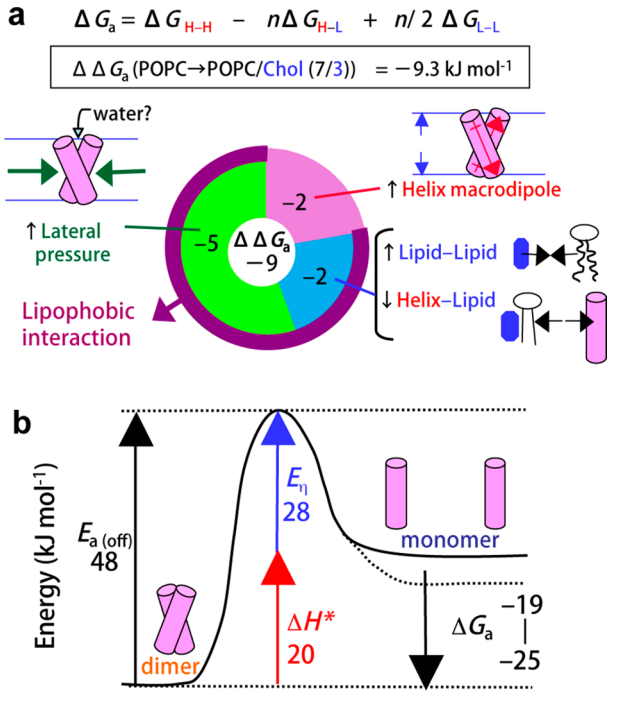

Figure 4. (a) Possible cholesterol-induced forces that drive association of the helices. In a latticelike contact model, the helix association energy in the bilayer can be decomposed into an increase in the level of helix−helix interactions ($+\Delta G_{H-H}$), a decrease in the level of helix−lipid interactions by removing n lipids ($-n\Delta G_{H-L}$), and an increase in the level of lipid−lipid interactions among the removed lipids ($+n/2\ \Delta G_{L-L}$). The free energy contributions that drive helix association via addition of cholesterol [$\Delta\Delta G_a$(POPC → POPC/cholesterol)] can originate from a stronger helix macrodipole attraction because of the lower polarity at the helix termini in thicker membranes (negative ΔG_{H-H}), unfavorable helix−cholesterol contact (positive ΔG_{H-L}), and favorable POPC−cholesterol contact (negative ΔG_{L-L}). In addition to these contact energies, helix association can also be driven by the release of curvature strain (lateral pressure) by the formation of an hourglass-shaped dimer. (b) Hypothetical reaction coordinate for helix dissociation. $E_{a(off)}$, E_η, ΔH^*, and ΔG_a represent the activation energy for dissociation, the activation energy for lipid diffusion, the activation enthalpy for protein dissociation (intrinsic energy barrier), and the association free energy change, respectively.

DOI: 10.1021/bi501528e
Biochemistry 2015, 54, 1371−1379

membranes,[57] the interfacial energies between a protein and membrane can be significant (>50 kJ mol^{-1}), depending on the tilt angle and shape of the dimers. The negative curvature of POPC/cholesterol (7/3) membranes is similar to that of POPC/POPE (1/1) membranes (−0.14 nm^{-1} at 25 °C).[58] The observed $\Delta\Delta G_a$(POPC → POPC/POPE) of approximately −6 kJ mol^{-1} at 25 °C[33] originates from both membrane thickening (27 → 28 Å) and the lateral pressure effect. The former contribution to $\Delta\Delta G_a$ should be small and roughly correspond to half of $\Delta\Delta G_a$ [diC (18:1) PC → diC (20:1) PC] (approximately −2 kJ mol^{-1}), in which the hydrophobic thickness increases from 27 to 30.5 Å (vide supra).[32] Therefore, the lateral pressure contribution was assumed to be approximately −5 kJ mol^{-1} for both the POPC/POPE and POPC/cholesterol membranes (Figure 4a). Of note, the lateral pressure profile can be significantly changed by the position of the unsaturated double bond of the phospholipid acyl chain, as reported by Cantor.[12] In PC/cholesterol mixtures, the PC profile change can further affect the overall profile by changing the position and orientation of cholesterol and, as a consequence, affect helix association. For example, moving the 18:1$_{\Delta 9}$ double bond of POPC toward the water−membrane interface (18:1$_{\Delta 6}$ or 18:1$_{\Delta 3}$) is expected to result in a pressure shift toward the interface, attenuating the cholesterol-induced association and/or tilt of the helices by partially conpensating for the higher pressure in the bilayer center.

Association−Dissociation Kinetics. Having confirmed that the smFRET and ensemble FRET measurements yield consistent results on helix dimerization, we obtained data on the activation energy for the dissociation of antiparallel dimers from the temperature dependence of smFRET trajectories [$E_{a(off)}$ = 48 kJ mol^{-1} (Figure 3e)]. Because it has been well-documented that the viscosity of the aqueous phase significantly affects the dynamics of proteins,[59,60] the membrane viscosity, which is 2 orders of magnitude higher than that in the aqueous phase, was assumed to be critical for the dynamic stability of membrane proteins. Although this concept was introduced in a review by Lee,[1] it has not been experimentally tested to the best of our knowledge. To examine the relationship between the lateral mobility of lipids and dynamics of helix dissociation, we measured the temperature dependence of diffusion coefficients (D_m) for fluorophore-labeled lipids in giant POPC/cholesterol vesicles by fluorescence correlation spectroscopy (Figure 8 of the Supporting Information). The activation energy originating from the membrane friction (E_η = 27.9 ± 1.4 kJ mol^{-1}) was obtained from the Arrhenius (Andrade) relation $D_m/T = A' \exp(-E_\eta/RT)$, where temperature-independent terms were included in pre-exponential factor A'.[61] The observed diffusion coefficients were consistent with those in previous studies.[62,63] The E_η value represents the Kramers-type frictional energy barrier.[1,61] Together with the enthalpic barrier of the dimer dissociation in the activated state ΔH^*, the observed rate constant k_{off} can be described as

$$k_{off} = A'' \exp(-\Delta H^*/RT) \times \exp(-E_\eta/RT) = A'' \exp[-E_{a(off)}/RT] \quad (3)$$

where $E_{a(off)} = \Delta H^* + E_\eta$. As shown in Figure 4b, the E_η value was comparable to the apparent excess energy in the dissociation process, indicating the absence of an enthalpically unfavorable transition state in the dissociation process ($\Delta H^* \approx -\Delta G_a$). Instead, the helix dissociation rate was strongly controlled by the dynamics of surrounding membranes (solvent-slaved process).[60] We hypothesized that the ΔH^* in the intermediate state (~20 kJ mol^{-1}) originated from the canceling out of the dipole−dipole interaction. If an interhelical distance of 1.0 nm is assumed in the dimer, formation of the intermediate state should require separation of the helices by ~0.6 nm (Figure 8 of the Supporting Information), which is comparable to the radius of lipids (~0.5 nm). The dimerization rate, k_{on}, did not show a clear temperature dependence (Figure 3d). However, this process is expected to have an activation energy, $E_{a(on)}$, represented by $E_{a(off)} + \Delta G_a$, with the second term being temperature-dependent (Figure 4b). Incorporating eq 2 into the Arrhenius equation results in

$$\ln k_{on} = -\frac{E_{a(off)} + \Delta G_a}{RT} = -\frac{E_{a(off)} + \Delta H_a - \Delta C_p T_{ref}}{RT} + \frac{\Delta C_p \ln(T/T_{ref})}{R} + \text{constant} \quad (4)$$

where we can simulate the temperature dependence using the thermodynamic parameters $E_{a(off)}$, ΔH_a, and ΔC_p (the constant term is the fitting parameter). The value of the slope, which is roughly equal to $-[E_{a(off)} + \Delta H_a]/R$, became positive because of the large negative value of ΔH_a (−84 kJ mol^{-1}) compared with the positive value of $E_{a(off)}$ (48 kJ mol^{-1}). The simulation reasonably described the data within the experimental errors (dashed line in Figure 3d). Note that the entropy contribution in the monomer−dimer interconversion cannot be described in the single-reaction coordinate.[1] Interestingly, the observed association rate (4−8 s^{-1}) was significantly slower than the theoretical collision rate[64] (~500 s^{-1}), assuming a vesicle diameter of 100 nm (corresponding to a bilayer circle with a radius of 100 nm), a critical radius r_c of 0.6 nm, and a diffusion coefficient D for helix **III** of 6.6 μm^2 s^{-1} (determined by FCS at 25 °C). The occasional dimer formation following collision suggests the presence of additional steric/orientational constraints for stable association,[64] consistent with the observed significant decrease in entropy upon association (vide supra). This is reasonable considering that the time scale of the helix−lipid rearrangement (>10−100 ns)[2] is comparable to that of the duration of interhelical contact in free diffusion (=$r_c^2/4D$ = 14 ns). Effective dimer formation may require specific helix configurations for the formation of the hourglass-shaped dimer.

CONCLUSIONS

The smFRET measurements in lipid vesicles revealed a new approach to monitoring association−dissociation dynamics of transmembrane helices in real time. We found that the dimer of the simplest model transmembrane helices could have lifetimes of subseconds in the presence of cholesterol. The dissociation rate was closely associated with the membrane dynamics (Figure 4b). The cholesterol-induced stabilizing energy (−9.3 kJ mol^{-1}) can be decomposed into a stronger dipole−dipole attraction (approximately −2 kJ mol^{-1}), the lateral pressure effect (approximately −5 kJ mol^{-1}), and contact energies of helix−POPC and POPC−cholesterol interactions (approximately −2 kJ mol^{-1}) (Figure 4a). The latter two contributions can be considered as cholesterol-induced "lipophobic" interactions between transmembrane helices (Figure 4a). We propose that cholesterol induces configurational restriction for the helix to form an hourglass-shaped dimer to release the higher lateral pressure in the hydrocarbon core, consistent with

DOI: 10.1021/bi501528e
Biochemistry 2015, 54, 1371−1379

experimental observations, such as a larger helix tilt, a positive $\Delta C_{p(a)}$, and limited dimerization after collisions. Such lipophobic forces by cholesterol (this study) and small-headgroup lipids[33] might be developed in the evolution process for stabilizing helical bundles in membrane environments as a counterpart of hydrophobic interaction in an aqueous environment. The liposomal smFRET approach described above will be useful for investigating the effects of not only membrane properties on helices but also sequence motifs such as the GXXXG motif on protein stability.

■ ASSOCIATED CONTENT

Supporting Information

Detailed methods of ensemble FRET and the synthesis of cross-linked helices, concentration dependence of the NBD fluorescence of **I**, ensemble NBD spectra, the number distribution of the helices in vesicles, lipid homogeneity, smFRET measurement with a defined relative orientation, additional smFRET data, lipid diffusion, and distance dependence of dipole−dipole interaction. This material is available free of charge via the Internet at http://pubs.acs.org.

■ AUTHOR INFORMATION

Corresponding Author

*Phone: +81-75-753-4521. Fax: +81-75-753-4578. E-mail: mkatsumi@pharm.kyoto-u.ac.jp.

Funding

This work was supported in part by Grants-in-Aid for Scientific Research on Innovative Areas (21107514), for Young Scientists (B) (18790025), and for Scientific Research (C) (25460034) from the Ministry of Education, Culture, Sports, Science and Technology of Japan.

Notes

The authors declare no competing financial interest.

■ ABBREVIATIONS

biotin-PE, 1,2-dipalmitoyl-*sn*-glycero-3-phosphoethanolamine-*N*-(cap biotinyl); DABMI, $NHCH_2CH_2$-S-*N*-(4-{[4-(dimethylamino)phenyl]azo}phenyl)-4′-maleimide; FTIR−PATR, Fourier transform infrared−polarized attenuated total reflection; FRET, fluorescence resonance energy transfer; LUVs, large unilamellar vesicles; NBD, 7-nitrobenz-2-oxa-1,3-diazole; PEG, poly(ethylene glycol); POPC, 1-palmitoyl-2-oleoyl-*sn*-glycero-3-phosphatidylcholine; smFRET, single-molecule fluorescence resonance energy transfer.

■ ADDITIONAL NOTE

[a]The flip-flop of this type of helix does not occur on a time scale of a day. See ref 38.

■ REFERENCES

(1) Lee, A. G. (2004) How lipids affect the activities of integral membrane proteins. *Biochim. Biophys. Acta 1666*, 62−87.

(2) Marsh, D. (2008) Protein modulation of lipids, and vice-versa, in membranes. *Biochim. Biophys. Acta 1778*, 1545−1575.

(3) Phillips, R., Ursell, T., Wiggins, P., and Sens, P. (2009) Emerging roles for lipids in shaping membrane-protein function. *Nature 459*, 379−385.

(4) Popot, J. L., and Engelman, D. M. (2000) Helical membrane protein folding, stability, and evolution. *Annu. Rev. Biochem. 69*, 881−922.

(5) Gimpl, G., Burger, K., and Fahrenholz, F. (1997) Cholesterol as modulator of receptor function. *Biochemistry 36*, 10959−10974.

(6) Baenziger, J. E., Morris, M. L., Darsaut, T. E., and Ryan, S. E. (2000) Effect of membrane lipid composition on the conformational equilibria of the nicotinic acetylcholine receptor. *J. Biol. Chem. 275*, 777−784.

(7) Cornelius, F. (2001) Modulation of Na,K-ATPase and Na-ATPase activity by phospholipids and cholesterol. I. Steady-state kinetics. *Biochemistry 40*, 8842−8851.

(8) Soubias, O., and Gawrisch, K. (2012) The role of the lipid matrix for structure and function of the GPCR rhodopsin. *Biochim. Biophys. Acta 1818*, 234−240.

(9) Zocher, M., Zhang, C., Rasmussen, S. G., Kobilka, B. K., and Muller, D. J. (2012) Cholesterol increases kinetic, energetic, and mechanical stability of the human β_2-adrenergic receptor. *Proc. Natl. Acad. Sci. U.S.A. 109*, E3463−E3472.

(10) Song, Y., Kenworthy, A. K., and Sanders, C. R. (2013) Cholesterol as a co-solvent and a ligand for membrane proteins. *Protein Sci. 23*, 1−22.

(11) Ikonen, E. (2008) Cellular cholesterol trafficking and compartmentalization. *Nat. Rev. Mol. Cell Biol. 9*, 125−138.

(12) Cantor, R. S. (1999) Lipid composition and the lateral pressure profile in bilayers. *Biophys. J. 76*, 2625−2639.

(13) Veatch, S. L., and Keller, S. L. (2003) Separation of liquid phases in giant vesicles of ternary mixtures of phospholipids and cholesterol. *Biophys. J. 85*, 3074−3083.

(14) Lingwood, D., and Simons, K. (2010) Lipid rafts as a membrane-organizing principle. *Science 327*, 46−50.

(15) Ren, J., Lew, S., Wang, Z., and London, E. (1997) Transmembrane orientation of hydrophobic α-helices is regulated both by the relationship of helix length to bilayer thickness and by the cholesterol concentration. *Biochemistry 36*, 10213−10220.

(16) Mall, S., Broadbridge, R., Sharma, R. P., East, J. M., and Lee, A. G. (2001) Self-association of model transmembrane α-helices is modulated by lipid structure. *Biochemistry 40*, 12379−12386.

(17) Smith, S. O., Song, D., Shekar, S., Groesbeek, M., Ziliox, M., and Aimoto, S. (2001) Structure of the transmembrane dimer interface of glycophorin A in membrane bilayers. *Biochemistry 40*, 6553−6558.

(18) Cristian, L., Lear, J. D., and DeGrado, W. F. (2003) Use of thiol-disulfide equilibria to measure the energetics of assembly of transmembrane helices in phospholipid bilayers. *Proc. Natl. Acad. Sci. U.S.A. 100*, 14772−14777.

(19) Sparr, E., Ash, W. L., Nazarov, P. V., Rijkers, D. T., Hemminga, M. A., Tieleman, D. P., and Killian, J. A. (2005) Self-association of transmembrane α-helices in model membranes: Importance of helix orientation and role of hydrophobic mismatch. *J. Biol. Chem. 280*, 39324−39331.

(20) Hong, H., and Bowie, J. U. (2011) Dramatic destabilization of transmembrane helix interactions by features of natural membrane environments. *J. Am. Chem. Soc. 133*, 11389−11398.

(21) White, S. H., and Wimley, W. C. (1999) Membrane protein folding and stability: Physical principles. *Annu. Rev. Biophys. Biomol. Struct. 28*, 319−365.

(22) Engelman, D. M., Chen, Y., Chin, C. N., Curran, A. R., Dixon, A. M., Dupuy, A. D., Lee, A. S., Lehnert, U., Matthews, E. E., Reshetnyak, Y. K., Senes, A., and Popot, J. L. (2003) Membrane protein folding: Beyond the two stage model. *FEBS Lett. 555*, 122−125.

(23) Lemmon, M. A., and Engelman, D. M. (1994) Specificity and promiscuity in membrane helix interactions. *Q. Rev. Biophys. 27*, 157−218.

(24) Killian, J. A. (1998) Hydrophobic mismatch between proteins and lipids in membranes. *Biochim. Biophys. Acta 1376*, 401−415.

(25) Nielsen, C., Goulian, M., and Andersen, O. S. (1998) Energetics of inclusion-induced bilayer deformations. *Biophys. J. 74*, 1966−1983.

(26) Cantor, R. S. (2002) Size distribution of barrel-stave aggregates of membrane peptides: Influence of the bilayer lateral pressure profile. *Biophys. J. 82*, 2520−2525.

(27) Russ, W. P., and Engelman, D. M. (1999) TOXCAT: A measure of transmembrane helix association in a biological membrane. *Proc. Natl. Acad. Sci. U.S.A. 96*, 863−868.

DOI: 10.1021/bi501528e
Biochemistry 2015, 54, 1371−1379

(28) Gurezka, R., and Langosch, D. (2001) In vitro selection of membrane-spanning leucine zipper protein-protein interaction motifs using POSSYCCAT. *J. Biol. Chem. 276*, 45580−45587.
(29) Li, E., Wimley, W. C., and Hristova, K. (2012) Transmembrane helix dimerization: Beyond the search for sequence motifs. *Biochim. Biophys. Acta 1818*, 183−193.
(30) Song, Y., Hustedt, E. J., Brandon, S., and Sanders, C. R. (2013) Competition between homodimerization and cholesterol binding to the C99 domain of the amyloid precursor protein. *Biochemistry 52*, 5051−5064.
(31) Senes, A., Engel, D. E., and DeGrado, W. F. (2004) Folding of helical membrane proteins: The role of polar, GxxxG-like and proline motifs. *Curr. Opin. Struct. Biol. 14*, 465−479.
(32) Yano, Y., and Matsuzaki, K. (2006) Measurement of thermodynamic parameters for hydrophobic mismatch 1: Self-association of a transmembrane helix. *Biochemistry 45*, 3370−3378.
(33) Yano, Y., Yamamoto, A., Ogura, M., and Matsuzaki, K. (2011) Thermodynamics of insertion and self-association of a transmembrane helix: A lipophobic interaction by phosphatidylethanolamine. *Biochemistry 50*, 6806−6814.
(34) Roy, R., Hohng, S., and Ha, T. (2008) A practical guide to single-molecule FRET. *Nat. Methods 5*, 507−516.
(35) Schuler, B., and Eaton, W. A. (2008) Protein folding studied by single-molecule FRET. *Curr. Opin. Struct. Biol. 18*, 16−26.
(36) Okumus, B., Wilson, T. J., Lilley, D. M., and Ha, T. (2004) Vesicle encapsulation studies reveal that single molecule ribozyme heterogeneities are intrinsic. *Biophys. J. 87*, 2798−2806.
(37) Bartlett, G. R. (1959) Phosphorus assay in column chromatography. *J. Biol. Chem. 234*, 466−468.
(38) Yano, Y., Takemoto, T., Kobayashi, S., Yasui, H., Sakurai, H., Ohashi, W., Niwa, M., Futaki, S., Sugiura, Y., and Matsuzaki, K. (2002) Topological stability and self-association of a completely hydrophobic model transmembrane helix in lipid bilayers. *Biochemistry 41*, 3073−3080.
(39) Joo, C., and Ha, T. (2012) Preparing sample chambers for single-molecule FRET. *Cold Spring Harbor Protocols 2012*, 1104−1108.
(40) Ha, T., and Tinnefeld, P. (2012) Photophysics of fluorescent probes for single-molecule biophysics and super-resolution imaging. *Annu. Rev. Phys. Chem. 63*, 595−617.
(41) McKinney, S. A., Joo, C., and Ha, T. (2006) Analysis of single-molecule FRET trajectories using hidden Markov modeling. *Biophys. J. 91*, 1941−1951.
(42) Heerklotz, H., and Tsamaloukas, A. (2006) Gradual change or phase transition: Characterizing fluid lipid-cholesterol membranes on the basis of thermal volume changes. *Biophys. J. 91*, 600−607.
(43) Nezil, F. A., and Bloom, M. (1992) Combined influence of cholesterol and synthetic amphiphillic peptides upon bilayer thickness in model membranes. *Biophys. J. 61*, 1176−1183.
(44) Salnikov, E. S., Mason, A. J., and Bechinger, B. (2009) Membrane order perturbation in the presence of antimicrobial peptides by ^{2}H solid-state NMR spectroscopy. *Biochimie 91*, 734−743.
(45) Uphoff, S., Holden, S. J., Le Reste, L., Periz, J., van de Linde, S., Heilemann, M., and Kapanidis, A. N. (2010) Monitoring multiple distances within a single molecule using switchable FRET. *Nat. Methods 7*, 831−836.
(46) Hern, J. A., Baig, A. H., Mashanov, G. I., Birdsall, B., Corrie, J. E., Lazareno, S., Molloy, J. E., and Birdsall, N. J. (2010) Formation and dissociation of M1 muscarinic receptor dimers seen by total internal reflection fluorescence imaging of single molecules. *Proc. Natl. Acad. Sci. U.S.A. 107*, 2693−2698.
(47) Kasai, R. S., Suzuki, K. G., Prossnitz, E. R., Koyama-Honda, I., Nakada, C., Fujiwara, T. K., and Kusumi, A. (2011) Full characterization of GPCR monomer-dimer dynamic equilibrium by single molecule imaging. *J. Cell Biol. 192*, 463−480.
(48) Suzuki, K. G., Kasai, R. S., Hirosawa, K. M., Nemoto, Y. L., Ishibashi, M., Miwa, Y., Fujiwara, T. K., and Kusumi, A. (2012) Transient GPI-anchored protein homodimers are units for raft organization and function. *Nat. Chem. Biol. 8*, 774−783.
(49) Karjalainen, E. L., and Barth, A. (2012) Vibrational coupling between helices influences the amide I infrared absorption of proteins: Application to bacteriorhodopsin and rhodopsin. *J. Phys. Chem. B 116*, 4448−4456.
(50) Benjamini, A., and Smit, B. (2012) Robust driving forces for transmembrane helix packing. *Biophys. J. 103*, 1227−1235.
(51) Joh, N. H., Min, A., Faham, S., Whitelegge, J. P., Yang, D., Woods, V. L., and Bowie, J. U. (2008) Modest stabilization by most hydrogen-bonded side-chain interactions in membrane proteins. *Nature 453*, 1266−1270.
(52) Meyer, B. H., Segura, J. M., Martinez, K. L., Hovius, R., George, N., Johnsson, K., and Vogel, H. (2006) FRET imaging reveals that functional neurokinin-1 receptors are monomeric and reside in membrane microdomains of live cells. *Proc. Natl. Acad. Sci. U.S.A. 103*, 2138−2143.
(53) Saito, H., Miyako, Y., Handa, T., and Miyajima, K. (1997) Effect of cholesterol on apolipoprotein A-I binding to lipid bilayers and emulsions. *J. Lipid Res. 38*, 287−294.
(54) Wimley, W. C., and White, S. H. (1993) Membrane partitioning: Distinguishing bilayer effects from the hydrophobic effect. *Biochemistry 32*, 6307−6312.
(55) Bocharov, E. V., Pustovalova, Y. E., Pavlov, K. V., Volynsky, P. E., Goncharuk, M. V., Ermolyuk, Y. S., Karpunin, D. V., Schulga, A. A., Kirpichnikov, M. P., Efremov, R. G., Maslennikov, I. V., and Arseniev, A. S. (2007) Unique dimeric structure of BNip3 transmembrane domain suggests membrane permeabilization as a cell death trigger. *J. Biol. Chem. 282*, 16256−16266.
(56) Angel, T. E., Gupta, S., Jastrzebska, B., Palczewski, K., and Chance, M. R. (2009) Structural waters define a functional channel mediating activation of the GPCR, rhodopsin. *Proc. Natl. Acad. Sci. U.S.A. 106*, 14367−14372.
(57) Dan, N., and Safran, S. A. (1998) Effect of lipid characteristics on the structure of transmembrane proteins. *Biophys. J. 75*, 1410−1414.
(58) Kollmitzer, B., Heftberger, P., Rappolt, M., and Pabst, G. (2013) Monolayer spontaneous curvature of raft-forming membrane lipids. *Soft Matter 9*, 10877−10884.
(59) Gavish, B., and Werber, M. M. (1979) Viscosity-dependent structural fluctuations in enzyme catalysis. *Biochemistry 18*, 1269−1275.
(60) Fenimore, P. W., Frauenfelder, H., McMahon, B. H., and Parak, F. G. (2002) Slaving: Solvent fluctuations dominate protein dynamics and functions. *Proc. Natl. Acad. Sci. U.S.A. 99*, 16047−16051.
(61) Frauenfelder, H., and Wolynes, P. G. (1985) Rate theories and puzzles of hemeprotein kinetics. *Science 229*, 337−345.
(62) Filippov, A., Oradd, G., and Lindblom, G. (2003) The effect of cholesterol on the lateral diffusion of phospholipids in oriented bilayers. *Biophys. J. 84*, 3079−3086.
(63) Kahya, N., and Schwille, P. (2006) How phospholipid-cholesterol interactions modulate lipid lateral diffusion, as revealed by fluorescence correlation spectroscopy. *J. Fluoresc. 16*, 671−678.
(64) Berg, O. G., and von Hippel, P. H. (1985) Diffusion-controlled macromolecular interactions. *Annu. Rev. Biophys. Biophys. Chem. 14*, 131−160.

DOI: 10.1021/bi501528e
Biochemistry 2015, 54, 1371−1379